

NMR evidence for very slow carrier density fluctuations in the organic metal (TMTSF)₂ClO₄

F. Zhang, Y. Kurosaki, J. Shinagawa, B. A. Lavi, and S. E. Brown
Department of Physics & Astronomy, UCLA, Los Angeles, California 90095

We have investigated the origin of the large increase in spin-echo decay rates for the ⁷⁷Se nuclear spins at temperatures near to $T = 30\text{K}$ in the organic superconductor (TMTSF)₂ClO₄. The measured angular dependence of T_2^{-1} demonstrates that the source of the spin-echo decays lies with carrier density fluctuations rather than fluctuations in TMTSF molecular orientation. The very long time scales are directly associated with the dynamics of the anion ordering occurring at $T = 25\text{K}$, and the inhomogeneously broadened spectra at lower temperatures result from finite domain sizes. Our results are similar to observations of line-broadening effects associated with charge-ordering transitions in quasi-two dimensional organic conductors.

(TMTSF)₂ClO₄ is a member of the Bechgaard salts family of organic conductors and superconductors. While the original discovery of organic superconductivity was made in the isostructural system (TMTSF)₂PF₆ at Orysay¹, the perchlorate salt was interesting because it was the only composition undergoing a superconducting transition ($T_c = 1.4\text{K}$) at ambient pressure^{2,3}. Another difference, when compared with the hexafluoride salts is that the counterion is non-centrosymmetric. As a result, there is a symmetry breaking of the high-temperature crystallographic space group (Pmma), when the ClO₄ counterions orientationally order at $T_{AO} = 25\text{K}$ with wavevector $Q = (0; 1/2; 0)$ ⁴. This particular Q leads to inequivalent TMTSF stacks and therefore also two bands crossing the Fermi energy E_F . Some of the low-temperature properties of (TMTSF)₂ClO₄ that differ from the PF₆ salt are attributed to this difference^{5,6,7,8}.

The phase transition at T_{AO} is a metal-metal phase transition driven by lattice Coulomb effects at which a disproportionation, or charge order (CO), of carrier density between the adjacent stacks accompanies the counterion ordering. By now, CO is known to be ubiquitous to the analog TMTTF-based salts with counterions ranging from hexafluorides like ASF₆ to non-centrosymmetric SCN or ReO₄. Those systems are all insulators, either resulting from the broken-symmetry of the CO phase transition itself^{9,10,11} or resulting from a dimerization of intrastack bond distances between TMTTF molecules^{12,13}. In the case of the insulators, there is little doubt that electron-electron interactions play a crucial role; nevertheless there is empirical evidence that coupling to the counterions allows the CO transition to take place. We examine the effects of the transition on the NMR properties as a window into what differences might be observed when compared to what is seen in the insulators.

Here we explore the effects of the anion ordering on the ⁷⁷Se NMR spectrum and relaxation in (TMTSF)₂ClO₄. In this case, the transverse spin relaxation rate is strongly affected by slow fluctuations of the electronic carrier density above T_{AO} . The slow fluctuations have been observed previously by Takigawa and Saito (TS)¹⁴, but with the difference that our experiments are done using single crystals, and we are able to demonstrate that

the carrier density fluctuations rather than molecular orientational fluctuations are responsible. The linewidth broadens homogeneously in association with these fluctuations and narrows on cooling further. From experiments undertaken below T_{AO} on quenched and relaxed samples, we conclude that the spectrum is dominated by disorder effects. This is very different from the insulators, where distinct symmetry-breaking signatures of the ordered phase are observed¹⁵. Even in the presence of the disorder, (TMTSF)₂ClO₄ is a superconductor, and the pairing is probably not s -wave.

The (TMTSF)₂ClO₄ crystals were grown using standard electrolysis techniques. In this case, the dimensions are $6.4\text{mm} \times 1.2\text{mm} \times 0.8\text{mm}$ and the mass is $m = 4.2\text{mg}$. Typically, crystals grow longer along the highly-conducting stack direction relative to the other directions. Our goal was to investigate the effect on the hyperfine fields resulting from the ClO₄ anion ordering, so the appropriate coil geometry is unusual when compared to most NMR investigations of the Bechgaard salts. We expected the hyperfine fields are principally dipolar¹⁴, arising from the p_z orbital on the Se atoms, extending out of the plane of the molecule. As a result, the strongest hyperfine fields are with the dc field aligned along the stacking axis, so we chose the symmetry axis of the coil to allow for sample rotations with the external field B_0 lying in the a - c plane. The AO transition occurs at $T_{AO} = 25\text{K}$, so we cooled at 40mK/min through it to reach the highly-conducting relaxed state.

Shown in Fig. 1 is the spin-echo decay rate T_2^{-1} (here we define T_2 as the time corresponding to $1/e$ decay) vs. temperature for several angles of the applied field $B_0 = 4.91\text{T}$. As observed by Takigawa and Saito¹⁴, we see a substantial increase in the relaxation rate on lowering the temperature through 30K . The questions we answer are how this increase in T_2^{-1} is related to anion ordering and the mechanism by which it occurs. By rotating the sample, we establish the anisotropy in T_2^{-1} in the vicinity of $T = 30\text{K}$. The size of the peak is found largest for the field applied along the stacking axis ($B_0 \parallel a$; $\theta = 0$), somewhat smaller for the c -direction, and even less when B_0 is rotated away from a by $\theta = 55^\circ$ (inset; also see Eq. 2 below, noting that $3\cos^2\theta - 1 = 0$), where

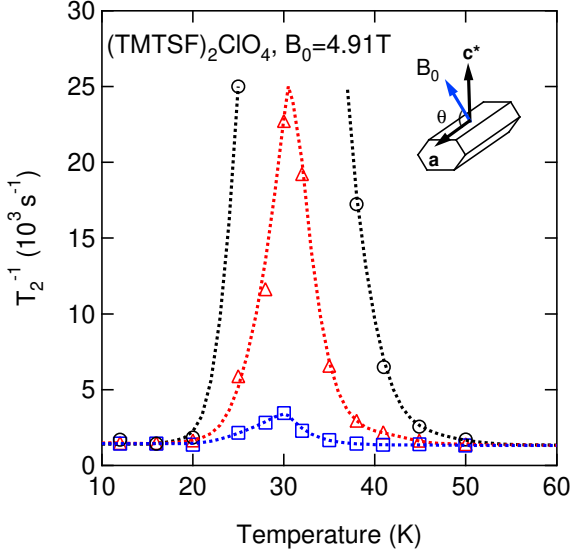


FIG. 1: (Color Online) Temperature dependence of T_2^{-1} for three orientations of the crystal relative to the external magnetic field. The inset illustrates the geometry. θ indicates the angle between the direction of applied field B_0 and a axis. The open circles are taken with $B_0 \parallel a$ ($\theta = 0$), the open triangles are taken with $B_0 \parallel c$ ($\theta = 90$), and the open squares are taken with $\theta = 45^\circ$. The dotted lines serve as guides to the eyes.

the anisotropic part of the hyperfine field vanishes. At the peak, the rate is too fast to allow for a measurement with the field along a .

A more complete angular dependence of the spin-echo decay rate is shown in Fig. 2 at $T = 38\text{K}$, where the relaxation rate is enhanced over a temperature-independent background. We also notice that there is a change in linewidth and lineshape on cooling through the temperatures where T_2^{-1} peaks. In the high temperature regime (i.e., $T > 50\text{K}$), the lineshape is very close to Gaussian. It changes to Lorentzian on the high-temperature side of the peak and returns to Gaussian (although considerably broader) on the low-temperature side of the peak.

In what follows, we make the case that the peak in T_2^{-1} vs. T is a result of the slowing down of carrier density

fluctuations linked to the inequivalence of TMTSF stacks developing at the anion ordering transition. The spin-echo decay is affected by the density fluctuations through the z component of the hyperfine fields, because local temporal variations result in dephasing of the precessing spins involved in a spin-echo experiment. To be more specific, suppose that a nuclear spin is situated in an environment in which the local field switches randomly between two discrete $\hbar\omega$ on a time scale τ_c . If this is the only source for the spin-echo decay, then the spin-echo amplitude decreases as

$$G(t) = G(0)e^{-(\hbar\omega)^2 \tau_c t}; \quad (1)$$

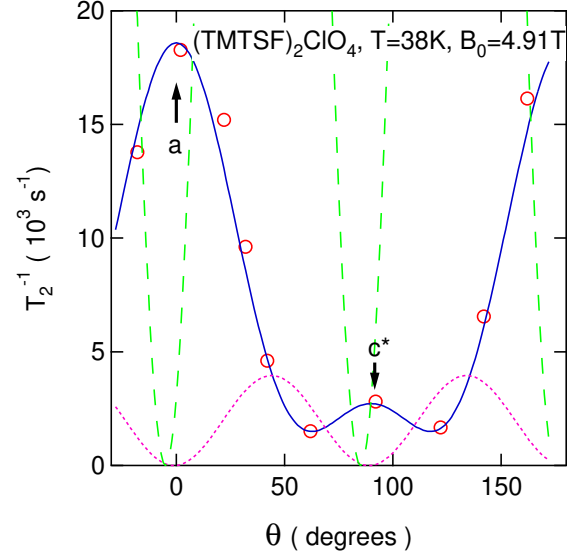


FIG. 2: (Color Online) Angular dependence of T_2^{-1} (red open circles) at $T = 38\text{K}$. The pink dotted line and the green dashed line are the expected angular dependence of T_2^{-1} in TSM model, corresponding to the molecular motion amplitudes of 2 and 10, respectively.

in the extreme narrowing limit ($\hbar\omega \ll 1$), with the gyromagnetic ratio. When Eq. 1 applies, the spectrum is said to be motionally narrowed. The spin-echo decay rate increases when $\hbar\omega$ grows larger, as it would on the approach to the anion ordering transition. Dephasing is most efficient when $\hbar\omega \approx 1$, where we expect a peak in T_2^{-1} . Below, we evaluate the form of the hyperfine coupling, and use it to describe the angular dependence of the spin-echo decay rate.

The angular dependence of the first moment as well as the spin-lattice relaxation rate T_1^{-1} at $T = 38\text{K}$ are shown in Fig. 3. We assume these are consistent with a uniaxial hyperfine coupling of the form

$$A(\theta) = A_{\text{iso}} + A_{\text{ax}}(3\cos^2\theta - 1); \quad (2)$$

$$K(\theta) = A(\theta)^{\frac{v}{2}}; \quad (3)$$

with v the volume per formula unit and s the dimensionless spin susceptibility. A_{iso} is the contribution from core polarization of the Se ions. We assume that A_{ax} is dominated by the intra-atomic Se p_z orbital and takes the form $A_{\text{ax}} = (2/5) \langle r^{-3} \rangle$ with the carrier density on a single ion. The upper limit for s is 0.25; it is reasonable to expect less, and TS used $s = 0.19$ calculated in Ref.¹⁶. The stacking (i.e., a) axis is very nearly coincident with the principal axis orthogonal to the plane of the TMTSF molecule.

Then the hyperfine field contribution to the spin-lattice relaxation rate also varies with angle, even though the spin susceptibility is isotropic¹⁷. For $B_0 \parallel a$ ($\theta = 0$) and

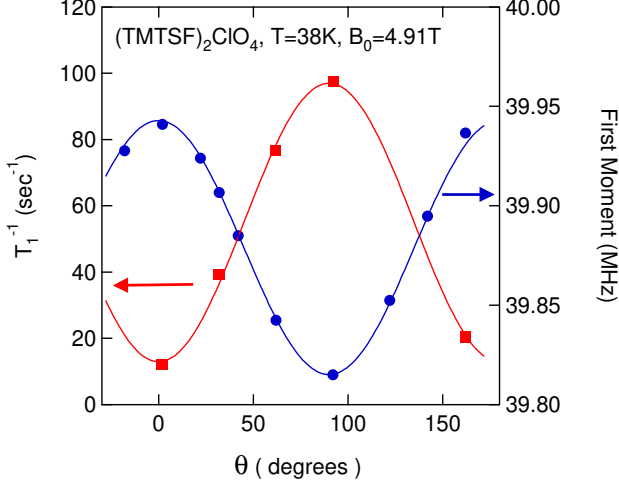


FIG. 3: (Color Online) First moment of the spectra (solid circles) and spin-lattice relaxation rate T_1^{-1} (solid squares) vs. angle at $T = 38\text{K}$.

where correlations are ignored, we have

$$\frac{1}{T_1^a T} = 4 \frac{k_B}{h} \frac{\gamma^2}{e} \frac{2\hbar}{e} (A_{\text{iso}} - A_{\text{ax}})^2 \frac{\gamma^2}{2} ; \quad (4)$$

with γ the gyromagnetic ratio of the free electron. For the angular dependence of the relaxation rate, we obtain

$$\frac{T_1^a}{T_1(\theta)} = \frac{(\gamma + 2)^2 \sin^2 \theta + (\gamma - 1)^2 (2 - \sin^2 \theta)}{2(\gamma - 1)^2} ; \quad (5)$$

where $\gamma = A_{\text{iso}}/A_{\text{ax}}$.

Inserting the accepted value for the spin susceptibility of $\chi_s = 1.6 \times 10^4 \text{ emu/mole(Fe)}^{17}$ into Eq. 3, together with $K_{\text{ax}} = 10.7 \times 10^4$ extracted from the angular dependence of the first moment (Fig. 3), we obtain a value for $\langle r^{-3} \rangle = 15a_0^{-3}$, where a_0 is the Bohr radius. This value is larger than the $9.3a_0^{-3}$ obtained for Se atoms from Hartree-Fock calculations¹⁸. The solid line running through the relaxation rate data shown in Fig. 3 is a least square fit to Eq. 5, from which we extract $\gamma = 0.37^{+0.09}$. Returning to Fig. 2 and using this value of γ , we obtain the solid line through the data points using the function

$$T_2^{-1} = \gamma^2 (K(\theta) B_0)^2 \tau_c(T) + B^2 ; \quad (6)$$

with B_0 the external applied magnetic field, and B a temperature and angle independent constant. The first term of Eq. 6 results from local field fluctuations originating in variations of the hyperfine coupling (Eq. 3), which are caused by carrier density fluctuations. At higher temperatures, τ_c is sufficiently short so as to make hyperfine field fluctuations inconsequential for the spin-echo decay, and it grows upon cooling with the slowing of the lattice fluctuations. γ is a constant that measures the amplitude of the hyperfine field fluctuations relative to the average.

Although the dependence of the spin-echo decay rate on the external field is the same as in TS model, the

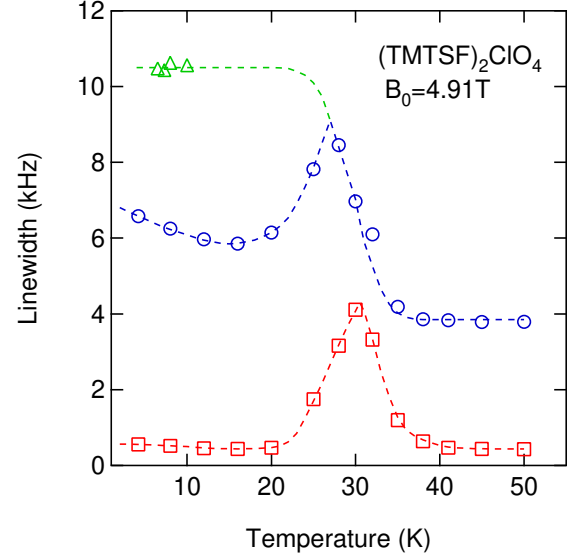


FIG. 4: (Color Online) Homogeneous and inhomogeneous linewidth as a function of temperature, taken with $B_0 = 4.91\text{T}$. The open circles are the inhomogeneous linewidth of the spectra, defined as the square root of the second moment. The open squares are the homogeneous linewidth, defined as the HWHM of the Fourier Transformation of the spin-echo decay. The triangles are the linewidth taken in the completely quenched state. The lines through the data points are guides to the eyes.

dependence on angle is very different to that expected for orientational fluctuations of the molecule. For contrast, we show the relative angular dependence of this mechanism for orientational fluctuation amplitudes of $\gamma = 2; 10$ in Fig. 2. In that case, the spin-echo decay rates induced by the local field fluctuations are largest where $dK/d\theta$ is maximum, namely near to θ_m . Instead, we observe a minimum at θ_m . The angular dependence is consistent with fluctuations in the hyperfine coupling, which includes the factor representing the fractional number of carriers per Se atom. Our interpretation is that as the correlation length for the counterion ordering grows, so does the characteristic time scale for the fluctuations in the usual way. In the ordered state there is an inequivalent carrier density on adjacent stacks, as a result of the period doubling of the lattice in the b direction. The fluctuations in the component of the hyperfine field parallel to the applied field follow. What is striking is that the time scales are governed by the lattice motion, while the hyperfine fields merely probe it.

The temperature dependence of the homogeneous and inhomogeneous linewidth for $B_0 = 4.91\text{T}$ is shown in Fig. 4, both in the relaxed and completely quenched state. At high temperatures, the spectra are dominated by the inhomogeneous broadening due to the inequivalent Se sites. The line is then homogeneously broadened on the high temperature side of the T_2^{-1} peak and is narrowed again on the low temperature side of the peak in the relaxed

state. At lower temperatures (below 10K), the inhomogeneous broadening grows significantly without evidence for saturation.

The fluctuation amplitude of the hyperne field can be estimated from the low temperature linewidth in the completely quenched state (Fig. 4) from which we obtain $\hbar\omega = 2 \approx 0 (10^4) \text{ Hz}$. Using this value of $\hbar\omega$ and $K (\approx 90) = 6.7 \cdot 10^4$, can be evaluated as 0.4. We can also estimate the characteristic time scale of the fluctuations near the peak to be $\tau_c = 0 (\frac{1}{2} \cdot 10^4) \text{ s}$. On the low temperature side of the peak of T_2^{-1} the fluctuations are so slow as to be ineffective in dephasing the transverse nuclear spin components in a spin-echo experiment. That we should observe this trend above T_{AO} should not be surprising because only on very slow cooling through the anion ordering transition results in a relaxed phase and superconductivity.

It remains to explain the nature of the low temperature inhomogeneous broadening in Fig. 4, which has a similar angular dependence as the homogeneous broadening peaking near 30K. Instead of two discrete peaks in the spectrum, there is a single broad feature. As a result of the anion ordering, there is a distinction between adjacent chains, say 'A' chains and 'B' chains. Zone folding produces two bands crossing the Fermi energy, where the degeneracy at the zone face near $(k_F; \approx 2b/q)$ is lifted by a small gap, Δ_{AO} . There is a corresponding difference in Fermi wavevector,

$$k_F = \frac{\Delta_{AO}}{\hbar v_F} \quad (7)$$

The two bands are of predominantly 'A' or 'B' character for these states near to the zone edge, but they are mixed if $k_F \approx 2$, with the correlation length of the counterion ordering measured along the stacks. Using $\Delta_{AO} \approx 2 \text{ meV}^{5,20}$ and $v_F = 2 \cdot 10^6 \text{ m/s}$ gives $k_F = 0 (10^{-3}) \text{ \AA}^{-1}$. Therefore, quite large values of Δ_{AO} are necessary to maintain the distinction between 'A' and 'B' chains. Perhaps sufficient order for observation of distinct chains could be achieved with slower cooling.

Indeed, in magnetotransport studies²⁰, much slower rates ($\approx 10 \text{ mK/min}$) were necessary to observe interference effects linked to the existence of the gap induced by the anion ordering²⁰.

If we presume the growth of the inhomogeneous broadening at low temperatures (Fig. 4) is linked to the configuration of the counterions, then either it is a dynamic effect linked to motional narrowing associated with lattice defect mobility, or it is a static effect, where the nature of the defects in the counterion sublattice changes as the temperature is lowered. For the latter, an example is where the domain boundary between 'A' and 'B' stacks broadens upon cooling, perhaps as a consequence of thermal contraction of the lattice. Experiments sensitive to spectral diffusion could distinguish between the two mechanisms for the broadening.

Finally, we make some general comments on our observations in the context of charge ordering in organic conductors. In our view, the reason for the very slow fluctuations evident here are the large masses and moments of inertia involved in the anion ordering transition. As a result of the coupling of the electronic states to the lattice potential, this becomes apparent in the spin-echo decay and inhomogeneous line broadening at low temperatures. Very similar results for spin-echo decays and inhomogeneous broadening were recently reported in ^{13}C NMR experiments on $-(\text{BEDT-TTF})_2\text{RbZn}(\text{SCN})_4$ ²¹, a quasi-two dimensional organic conductor. In that case, there is strong evidence that the slow fluctuations are directly associated with a charge-ordering phase transition, also linked to metal-insulator transition, for the 1/4-filled system. We suggest that the slow fluctuations are evidence that coupling to the lattice is an important component of the CO transition in that system, and perhaps all of the quasi-two dimensional organic systems undergoing charge order symmetry breaking.

This work was supported by the National Science Foundation under grant No. DMR-0203806. We acknowledge helpful discussions with Serguei B. Razovskii.

fzhang@physics.ucla.edu

- ¹ D. Jerome, A. Mazaud, M. Ribault, and K. Bechgaard, J. Phys. (Paris) Lett. 41, L95 (1980).
- ² S. S. P. Parkin, M. Ribault, D. Jerome, and K. Bechgaard, J. Phys. C 14, L445 (1981).
- ³ T. Ishiguro, K. Yamaji, and G. Saito, Organic Superconductors, Solid-state sciences (Springer-Verlag, New York, 1998).
- ⁴ J. P. Pouget and S. Ravy, J. Phys. I (France) 6, 1501 (1996), (review paper).
- ⁵ A. G. Lebed, N. N. Bagmet, and M. J. Naughton, Phys. Rev. Lett. 93, 157006 (2004).
- ⁶ W. Kang, S. T. Hannahs, and P. M. Chaikin, Phys. Rev. Lett. 70, 3091 (1993).
- ⁷ E. I. Chashechkina and P. M. Chaikin, Phys. Rev. B 56,

13658 (1997).

- ⁸ E. I. Chashechkina and P. M. Chaikin, Phys. Rev. Lett. 80, 2181 (1998).
- ⁹ H. Seo and H. Fukuyama, J. Phys. Soc. Japan 66, 1249 (1997).
- ¹⁰ D. S. Chow, F. Zamorszky, B. A. Lavi, D. J. Tantillo, A. Baur, C. A. Merlic, and S. E. Brown, Phys. Rev. Lett. 85, 1698 (2000).
- ¹¹ P. Monceau, F. Y. Nad, and S. B. Razovskii, Phys. Rev. Lett. 86, 4080 (2001).
- ¹² V. J. Emery, R. Bruinsma, and S. Barisic, Phys. Rev. Lett. 48, 1039 (1982).
- ¹³ D. Jerome and H. J. Schulz, Adv. Phys. 51, 293 (2002).
- ¹⁴ M. Takigawa and G. Saito, J. Phys. Soc. Japan 55, 1233 (1986).

- ¹⁵ F. Zam borszky, W . Yu, W . Raas, S. E. Brown, B. A lavi, C. A. M erlic, and A. Baur, J. Phys. IV France 12, 139 (2002).
- ¹⁶ R. M . M etzger, J. Chem . Phys. 75, 482 (1981).
- ¹⁷ M . M iljak, J. R. Cooper, and K. Bechgaard, Phys. Rev. B 37, 4970 (1988).
- ¹⁸ S. Fraga, K. M . S. Saxena, and J. K arowski, Handbook of atom ic data (Elsevier, Am sterdam , 1976).
- ¹⁹ The measured spin-lattice relaxation rate is faster than what is predicted using Eq. 4, and also that predicted in Ref.^{22,23} where it is argued that one-dim ensional param - agnons are responsible for the relaxation.
- ²⁰ S. U ji, T. Terashim a, H. A oki, J. S. B rooks, M . Tokum oto, S. Takasaki, J. Yam ada, and H. A nzai, Phys. Rev. B 53, 14399 (1996).
- ²¹ R. Chiba, K. Hiraki, T. Takahashi, H. M . Yam am oto, and T. Nakam ura, Phys. Rev. Lett. 93, 216405 (2004).
- ²² C. Bourbonnais, J. Phys. I France 3, 143 (1993).
- ²³ P. W zietek, F. Creuzet, C. Boumonnais, D. Jerome, K. Bechgaard, and P. Batail, J Phys. I France 3, 171 (1993).